Title

COSMIC-RAY-PRODUCED NEUTRONS ON THE GROUND: NEUTRON PRODUCTION RATE AND FLUX DISTRIBUTION

Authors

Yamashita, Mikio
Stephens, Lloyd D.
Patterson, H.Wade.

Publication Date

1966-01-12

UNIVERSITY OF CALIFORNIA
Lawrence Radiation Laboratory
Berkeley, California

AEC Contract No. W-7405-eng-48

COSMIC-RAY-PRODUCED NEUTRONS ON THE GROUND: NEUTRON PRODUCTION RATE AND FLUX DISTRIBUTION

Mikio Yamashita, Lloyd D. Stephens, and H. Wade Patterson

January 12, 1966

DISCLAIMER

Cosmic-Ray-Produced Neutrons on the Ground: Neutron Production Rate and Flux Distribution

Mikio Yamashita, Lloyd D. Stephens, and H. Wade Patterson

Lawrence Radiation Laboratory
University of California
Berkeley, California

January 12, 1966

ABSTRACT

The absolute rates of cosmic-ray neutron production and neutron flux distribution on the ground were determined at sea level and mountain altitude at a geomagnetic latitude $\lambda = 44°$ N in 1964. The thermal-neutron flux was measured with a well-calibrated BF_3 counter; a Maxwellian energy distribution with a shifted neutron temperature was assumed. By using two differently moderated BF_3 counters, the fast-neutron flux was determined in the energy range 0.4 eV to 10 MeV. The neutron fluxes were also estimated from the measured production rate, with good agreement with the measured fluxes; possible occurrence of air-ground boundary effects on the neutron flux distribution was considered. Anisotropy of the thermal-neutron flux on the ground was experimentally demonstrated, and the angular distribution was well filled by the first two terms of a spherical-harmonics expansion. The air-ground boundary effects are discussed on the basis of experimental results.

1. INTRODUCTION

Primary cosmic-rays, on entering the atmosphere, interact with air nuclei to cause disintegration secondaries such as neutrons, protons, pions, and other particles. Some of the secondaries possess enough energy to cause further disintegrations, thereby in turn creating nuclear cascades. Most cosmic-ray neutrons are thought to be produced by these high-energy nuclear interactions and by evaporation of neutrons from excited nuclei but the possibility of contributions from solar neutrons has been suggested recently [Lingenfelter and Flamm, 1964]. It has been shown that a major fraction of the total cosmic-ray-produced neutron flux comes from the evaporation process, having a roughly Maxwellian energy distribution peaked at about 1 MeV. To a lesser extent, direct interaction of high-energy radiations will produce neutrons of energies from about 1 MeV up to more than 1 BeV [Hess et al., 1961]. The neutrons produced initially in the atmosphere are slowed down rapidly by elastic and inelastic scattering, and therefore do not diffuse far from their point of origin before they are captured via $^{14}N(n,p)^{14}C$ reactions. Hence, since the neutron-producing radiations attenuate more slowly, neutron equilibrium with neutron-producing radiations is attained near the top of the atmosphere, as first shown by Bethe et al. [1940]. In the equilibrium region, referred to as the free atmosphere, the neutron absorption rate is equal to the neutron production rate and the neutron energy spectrum is independent of altitude. On the other hand, in the vicinity of the air-ground boundary, the energy and spatial distribution of cosmic-ray neutrons should be quite different from that in the free atmosphere, because of discontinuous change of the slowing-down properties and the rate of neutron production between air and earth. Accordingly, there is no more neutron equilibrium between the neutron production rate and the neutron absorption rate near the boundary. The effect of the boundary on the cosmic-ray neutron distribution was first investigated on theoretical grounds by Bethe et al. [1940]. They demonstrated the boundary effect in the case of an extended water surface. Their results show that immediately above the water surface a larger number of thermal neutrons is observed than in the free atmosphere, while the density of fast neutrons is reduced to about 20% of that in the free atmosphere. The results also indicate that there is a marked increase in the thermal-neutron density in the top 20 cm of water, caused by fast neutrons that are produced in air and diffuse into the water. As an experimental confirmation of a surface effect, Swetnick [1954] measured the thermal neutrons in water. His experimental results show that the top 30 cm of water is a transition region wherein the thermal-neutron intensity varies rapidly with depth. The rapid decrease of the thermal-neutron intensity between the 3- and 30-cm level agrees with theory, as he claimed. Below the 30-cm level, the thermal-neutron intensity is found to remain almost constant over the next 20 cm of water. Edge [1959] also measured the cosmic-ray slow neutrons and found nearly the same tendency of the slow-neutron intensity with depth as that obtained by Swetnick except in the first 5-cm layer; that is, a rapid decrease of slow-neutron intensity with depth in the first 20-cm layer and a slower decrease at greater depth.

However, such a distribution of slow neutrons below the water surface is questionable when we consider the neutron production absorption ratio on the whole in the nonequilibrium region near the water surface.

In this paper, our primary interest is determination of the absolute intensities of low-energy neutrons produced by the cosmic rays near the ground, because we feel there is a serious lack of experimental data in this area. Although several experimental data have been reported on ground-flux intensities [Kaplan et al., 1952, Boella et al., 1963, Hess et al., 1959, Kent, 1963, and Kästner et al., 1964], there exists a great discrepancy among them. Quantitative measurements of the cosmic-ray neutron fluxes on the ground are difficult because (1) the neutron-energy distribution is uncertain, (2) the air-ground boundary effects on the spatial and energy distribution of the neutrons depend greatly upon the type of local surroundings and (3) it is difficult to determine precisely the detection efficiency and energy dependence of the neutron detectors. On the other hand, the cosmic-ray neutron intensity should be related to the rate of production of neutrons within the scope of the variety of the air-ground boundary effects.

Since the neutron-producing radiations are of high energy and are directed predominantly in the forward direction, we expect that there is no air-ground boundary effect on the neutron producing radiations. In other words, neutron production in both air and earth in the vicinity of the boundary should be caused by the neutron-producing radiations of the same energy spectrum. Therefore, if we know the absolute neutron production rate, we can predict the neutron flux intensity at a certain location with an accuracy governed by the knowledge of the air-ground boundary effect and the local conditions for neutron diffusion. In this paper, we present our experimental results on the neutron flux intensities and production rate and compare the measured neutron fluxes with those calculated from the production rate. In addition, we discuss the air-ground boundary effects on the neutron distribution based on the experimental data. All experimental data were taken at White Mt. (10 600 ft), California, geomagnetic latitude $\lambda = 44°$ N, during August 1964, and at sea level in the vicinity of Berkeley, California, during July through December 1964.

2. MEASUREMENT OF COSMIC-RAY NEUTRON PRODUCTION RATE

To date, many experiments have been reported on the absolute rate of neutron production. One type of experiment uses 1/v detectors with known sensitivity to measure the slow-neutron flux in the free atmosphere, where the neutron absorption rate is balanced by the neutron production rate [Davis, 1950 and Yuan, 1951]. This sort of experiment determines the rate of production of neutrons that escape resonance absorption and reach the 1/v region. The experimental results thus obtained have been compared, with good agreement, with the concentration of ^{14}C produced by neutron capture in the atmosphere [Ladenburg, 1952 and Anderson, 1953]. The neutron production rate in a certain material on the ground also can be measured if the rate of production equals that of absorption in the material. This condition is created, for example, within a mass of material such as water or paraffin, the dimensions of which are large compared with the mean free path of the neutrons produced. Korff et al. [1948] first attempted such an experiment, and extensive studies were reported by several investigators [Tobey, 1949; Tobey and Montgomery, 1951; Lattimore, 1951; Swetnick, 1954].

Our experiments on the rate of neutron production were similarly made in water and in a paraffin pile. According to Tobey et al. [1951] a 63.5-by 63.5-by 92-cm paraffin pile was large enough to establish neutron equilibrium in it. Experimental results on slow-neutron distribution in water made by Swetnick [1954] showed that the slow-neutron intensity decreases rapidly with depth and reaches equilibrium at about 30 cm deep. In the equilibrium region, where the neutron production rate is equal to the rate of absorption, the relationship between the counting rate of a 1/v detector and the rate of neutron absorption in the medium is expressed as [Bethe et al., 1940]

$$q = \frac{R}{V} \cdot \frac{\tau_B}{\tau} \cdot \frac{1}{\rho} , \tag{1}$$

where q is the number of neutrons per gram per second absorbed at the 1/v region in the medium, ρ is the density of the medium, τ_B and τ are the mean lives of neutrons in the 1/v detector and the medium, respectively, R is the counting rate per second of the detector, and V is the volume of the detector in cm^3. In the above expression we have assumed a 1/v variation of the absorption cross section of the medium. Actually, two major corrections are necessary for Eq. (1). First, since the slow-neutron flux around the detector in a relatively nonabsorbing medium would be more or less depressed because of strong absorption of neutrons by the detector, the detector would see a smaller neutron flux than the equilibrium flux in the medium. Therefore the final result would be underestimated, unless properly corrected for the flux-depression effect. Second, the effective sensitivity of a 1/v detector for slow neutrons is usually different from the calculated one. For a $^{10}BF_3$ proportional counter, for example, the difference arises from the self-shielding effect, neutron absorption in the counter wall, an error in the ^{10}B content in the counter, and other minor factors. These facts necessitate an experimental correction to the sensitivity of the detector. Equation (1), corrected for the effects mentioned above, may be written as

$$q = \frac{R}{V} \cdot \frac{\tau_B}{\tau} \cdot \frac{1}{\rho} \cdot \frac{1}{\gamma} \cdot \frac{1}{f} , \tag{2}$$

where γ is the ratio of effective sensitivity of the detector to that calculated, and f the flux-depression factor.

A. Measuring Equipment and Calibration

We used a BF_3-gas-filled proportional counter for measurement of slow neutrons. The detector has an effective volume of 4.75-cm diam by 24.1-cm long, which is filled at a pressure of 20 cm Hg at 0° C with 96%-^{10}B-enriched BF_3. The 0.16-cm-thick cathode wall is 28% chromium and 72% iron. The counter was used at the center of the plateau of the operating-voltage curve--about 2800 V. The bias setting was such that gamma discrimination was proved in a gamma-ray field of 1.5 r/hr from ^{124}Sb with a negligibly small loss of pulses due to $^{10}B(n,\alpha)$ events.

The effective sensitivity of the BF_3 counter for an isotropic slow-neutron flux was measured by comparison with a calibrated In foil. A thin In foil was first calibrated in the thermal column of the LPTR at the Lawrence Radiation Laboratory, Livermore. Then the foil and the BF_3 counter were exposed to an isotropic flux of slow neutrons in a cavity within a thick concrete cube. The slow neutrons were produced by a Pu-Be source within the cavity [Patterson and Wallace, 1958]. The Cd-difference method was employed in calibrating both the BF_3 counter and the In foil. The advantage of this method is that since the capture cross section of indium for slow neutrons can be approximated by the 1/v curve below the ≈ 0.4-eV Cd cutoff [Hughes and Schwartz, 1958], both the In foil and the BF_3 counter may be regarded as 1/v detectors. Hence the relative sensitivity of both detectors for slow neutrons is independent of the energy distribution of the neutrons, as measured by means of the Cd-difference method. Experimental details and results are given elsewhere [Yamashita et al., 1965]. The effective total cross section of the BF_3 counter thus determined for an isotropic slow-neutron flux with a Maxwellian distribution at 20° C is 9.05 cm^2 with an estimated error of about 10%, while the Maxwellian average cross section calculated from the content of ^{10}B and its capture cross section is 10.36 cm^2.

B. Experiment and Results

The rate of production of cosmic-ray neutrons was measured in water and in a paraffin pile at the University of California's White Mountain High-Altitude Research Station (10 600 ft). Rates in water were measured at the deepest part (about 150 cm) of a small pond. The BF_3 counter, tightly covered with a thin polyethylene sheet, was suspended about 100 cm from the shore at a depth of 40 cm. According to the experimental results of Śwetnick [1954], neutron equilibrium is attained here. In the case of the paraffin pile, the BF_3 counter was placed at the center of the 60- by 69- by 96-cm pile with a negligibly small air gap between the counter and paraffin.

At sea level, experiments were also performed in both water and the paraffin pile. Measurements in water were carried out in a private swimming pool with a depth of about 3 m, while the paraffin pile employed was 90 by 100 by 105 cm. Since, in either case, the counting rates were very low, background events significantly contributed to the total counting rate. The background counts, caused by a contamination of the counter wall and to a lesser extent by cosmic-ray bursts or recoil events were determined by placing the BF_3 counter covered with a Cd sheet in a paraffin pile. This test was made at sea level and at the mountain altitude. There is no significant difference between the results at the two altitudes, indicating a negligibly small contribution from cosmic rays to the background. It should be mentioned that, although the net counting rates in water and paraffin were taken virtually by means of the Cd difference, this does not introduce a significant error because of the negligibly small neutron capture in the energies above the Cd cutoff.

The degree of flux depression around the counter in water or in the paraffin pile was experimentally evaluated. Counting rates were compared for two gemoetrically identical BF_3 counters, one of which was 96% ^{10}B enriched and the other 10% ^{10}B depleted. These were embedded in turn in the paraffin pile with a Pu Be neutron source on its surface. Relative sensitivity of the two counters under no flux-depression effect was determined in the air by comparing the counting rates against slow neutrons from a paraffin-moderated neutron source.

The flux-depression effect for the depleted counter in a diffusing medium could be reasonably neglected, and a decrease of the relative counting rate of the enriched counter in paraffin should be attributable to the flux-depression effect. The experimental procedures and necessary corrections to reduce the final results are described elsewhere [Yamashita et al., 1965]. The flux-depression factor thus obtained for the enriched BF_3 counter is about 0.95 in paraffin with no air gap between the counter and paraffin. This indicates a smaller flux-depression effect than the value calculated by Draper's formula for the case of an infinitely long cylinder [Draper, 1950]. It should be mentioned that an air-gap between the counter and the surrounding medium should considerably reduce the flux-depression effect. In what follows, we assume that the flux-depression factor in water is the same as that estimated experimentally in paraffin.

The experimental data on cosmic-ray neutron intensity could also be subject to small fluctuations in the neutron-producing radiations caused by a change of barometric pressure or primary cosmic-ray intensity. During the measurements at 10 600 ft elevation, a neutron monitor comprising a ^{10}B-enriched BF_3 counter covered with 2 in.-thick paraffin moderator was installed on the roof of a cottage to monitor the intensity of neutron-producing radiations in terms of fast-neutron flux. The neutron monitor showed no significant diurnal variation within the statistical error. Therefore we treat the experimental data by correcting only for a change of barometric pressure. The correction for barometric pressure, although generally less than the systematic errors introduced by experimental procedures, was made by using

$$A(p_0) = A(p) \exp\left(\frac{p-p_0}{L}\right) , \quad (3)$$

where $A(p)$ is the measured counting rate at a barometric pressure p (g/cm^2), and $A(p_0)$ is the corrected counting rate at the standard pressure p_0 at the measuring location. The attenuation length L for the neutron-producing radiation was taken equal to the generally accepted value of 145 g/cm^2 at a low altitude [Simpson et al., 1953]. Standard pressure p_0 was taken as 700 g/cm^2 at 10 600 ft, and 1030 g/cm^2 at sea level. The experimental results on the neutron production rate, corrected for barometric pressure, are shown in Table 1.

To obtain the neutron production rate in neutrons per second per gram from the measured counting rates, Eq. (2) was rewritten for water as

$$q = 1.90 \times 10^{-3} R \gamma^{-1} f^{-1} \quad (4a)$$

and for paraffin as

$$q = 2.71 \times 10^{-3} R \gamma^{-1} f^{-1} , \quad (4b)$$

where we use $V = 428$ cm^3, a thermal capture cross section of 0.33 barn for hydrogen and 4010 barn for ^{10}B, a density of 1 g/cm^3 for water and 0.9 g/cm^3 for paraffin, $\gamma = 0.874$ and $f = 0.95$, as described previously, and R is the measured counting rate in counts per second. In water, the oxygen atom is responsible for neutron production, while the carbon atom is in paraffin. According to experimental results on cosmic-ray neutron production rates in various elements [Tongiorgi, 1949; Simpson and Uretz, 1953; Brown, 1954; Ortel, 1954; Geiger, 1956], one can approximate the total neutron production rate per gram of an element of atomic weight A by

$$q = \text{const} \cdot A^{1/3} . \tag{5}$$

This empirical formula gives a relative rate of total neutron production in water, paraffin, air, and earth as shown in Table 2, where the composition of the media is assumed to be as indicated in the table. As shown in Table 1, the difference between the counting rates in water and the paraffin pile at 10 600 ft. elevation is considerably larger than expected from Table 2. This is considered to be due to the fact that the paraffin pile used there was not large enough to establish neutron equilibrium, hence allowing a significant contribution from neutrons produced outside the paraffin pile. In connection with this, the following experiment was carried out at the laboratory to estimate the effect of external neutrons on the 60- by 69- by 90-cm paraffin-pile system. Three radioactive neutron sources with well-known emission rates were placed at various positions on the surface of the pile, and neutrons were counted each time. Since the neutron sources were known to emit neutrons nearly isotropically, the counting rates integrated over the surface of the pile should correspond to the contribution to the pile from the external, isotropic neutron flux with an intensity equal to the emission rate of the neutron source used. The experimental results are summarized in Table 3.

As will be shown later, the intensity of fast-neutron flux on the ground at 10 600 ft elevation was about 7.5×10^{-2} n/cm^2-sec. This external neutron flux would have added 8.1, 5.1, and 1.6 cpm to the paraffin pile system if the neutron energy spectrum resembled that of Pu-Be, Po-mock fission, and Pu-Li, respectively. On the other hand, since no contribution from external neutrons to the counter in water was reasonably assumed, the difference between the counting rates measured in water and in the paraffin pile, taking into account the relative neutron production rates in both media, could be accounted for by the contribution from external neutrons to the paraffin pile. In this way, the contribution of external neutrons in counting rate to the paraffin pile at the White Mt. experiment was found to be 3.8 cpm. This result combined with a measured fast-neutron flux of 7.5×10^{-2} n/cm^2-sec and the data in Table 3 leads to an estimated average energy of 0.9 MeV for cosmic-ray fast neutrons on the ground. Although at sea level a larger bulk of paraffin was employed, the experimental results indicate that there might still be a small contribution from external neutrons to the paraffin-pile system.

Since the neutron production rate was measured in the medium, a correction is necessary for attenuation of the neutron-producing radiations during passage through the medium above the counter. For a mean free path of 145 g/cm^2 for attenuation of the neutron-producing radiations in the atmosphere and a geometric cross section [Brown, 1954], the neutron production rates at 40- and 50-cm depths in water were found to be 73.2 and 67.7%, respectively, of that at the water surface. Therefore, the corrected neutron production rates in water were found to be 1.28×10^{-4} n/g-sec at 700 g/cm^2 and 1.85×10^{-5} n/g-sec at sea level, as shown in Table 1.

3. MEASUREMENT OF NEUTRON FLUX

A. Experimental Method

During the experiment on neutron production rates, data were also taken on flux intensities of slow and fast neutrons on the ground. For slow neutrons, the same BF_3 counter as described previously was used, while the counter for measurement of fast-neutron fluxes was enveloped by two different moderators covered with a Cd sheet. The moderators were 0.9-in.-thick polyethylene and 2-1/2-in.-thick paraffin. The former was chosen because it was considered to have a satisfactorily flat response over intermediate energy regions; the latter supposedly was most suitable for measurement of neutrons with energies from 0.1 to 10 MeV. The energy dependence of the sensitivity of these moderated counters for directional neutron fluxes was determined experimentally from 1 eV to 10 MeV. However, since the spatial distribution of the fast-neutron flux on the ground is considered to be rather isotropic, the angular dependence of the sensitivity of the moderated counter must be determined. This was also determined experimentally by using various radioactive neutron sources of different energies. Details of the experiment are described elsewhere [Yamashita et al., 1965]. Combining the energy dependence curve of sensitivity for directional flux with data on the angular dependence, we obtained the response curve of the moderated counters with neutron energy for isotropic fast-neutron flux as shown in Fig. 1. The absolute sensitivity of the moderated counters was determined at energies of 25 keV and 4.2 MeV by using SbBe and PuBe neutron sources with well-known emission rates. Since the moderated counters do not have flat responses over the energy range of interest (1 eV to 10 MeV), an accurate measurement of fast-neutron flux requires information on the neutron energy spectrum. The energy spectrum of cosmic-ray neutrons has been investigated experimentally by Miyake et al. [1957] and Hess et al. [1959]. Hess et al. [1961] have theoretically treated the neutron energy spectrum by using multigroup diffusion theory. Newkirk [1963] has also calculated the energy distribution by means of the numerical multigroup Sn method. From the results of these investigations, we can describe approximately the energy distribution of low-energy neutrons in the free atmosphere as follows. The neutron flux intensity per unit energy interval decreases with energy as E^{-1} from 1 eV up to about 0.1 MeV, owing to elastic scattering with little absorption in the slowing-down process. At the energy region between 0.1 MeV and 1 MeV, the energy spectrum has a bump due to neutron evaporation. Above 1 MeV, the flux intensity decreases rapidly with energy. The reported results of the energy distribution are considerably different in the energy region from 0.1 to 10 MeV. Recently, Mendell et al. [1963] approximated the differential energy spectrum in n/cm^2-sec-MeV between 1 and 10 MeV by a power law of the form

$$\phi(E) = \text{const} \cdot E^{-n} \qquad (6)$$

and compared their experimental results obtained by balloon flights with the reported ones to show that n ranges from 1.16 to about 1.74, as shown in Table 4. The energy distribution of thermal neutrons in the atmosphere has been theoretically treated by several investigators and reviewed by Hess et al. [1959]. Although the results do not differ appreciably from each other, the expression based on theory for a heavy, gaseous moderator given by Poole et al. [1958] is supposedly the best approximation. However, it should be noted that the energy distribution of thermal neutrons described above is valid only in the free atmosphere.

In the vicinity of the air-ground boundary, the boundary effect should be governed by the fact that the earth has a smaller absorption cross section for slow neutrons and a larger slowing-down power than air. Thus, the lower energy part of the neutron spectrum should be more subject to the boundary effect.

To obtain the fast-neutron fluxes from the counting rates measured by two differently moderated detectors, we assume the following neutron energy spectrum in n/cm^2-sec-MeV on the ground in the energy range from 0.4 eV to 10 MeV:

$$\begin{aligned} \phi(E) &= C_1/E, & (0.4\ \text{eV} \leq E \leq 0.1\ \text{MeV}) \\ &= C_3 + C_4 E & (0.1\ \text{MeV} \leq E \leq 1\ \text{MeV}) \\ &= C_2 E^{-n} & (1\ \text{MeV} \leq E \leq 10\ \text{MeV}). \end{aligned} \tag{7}$$

Here C_1, C_2, C_3, C_4, and n are constants, C_3 and C_4 are expressed in terms of C_1 and C_2 from the continuity of the spectrum at 0.1 and 1 MeV, and C_1 and C_2 are to be determined from the counting rates in the following way.

The observed counting rate, R, is given by

$$R = \int_{0.4\ \text{eV}}^{10\ \text{MeV}} \phi(E)\,\eta(E)\,dE, \tag{8}$$

where $\eta(E)$ is the absolute sensitivity as a function of energy of the moderated detectors for an isotropic flux. This sensitivity is obtained for both the 0.9-in.-polyethylene- and 2-1/2-in.-paraffin-moderated detectors from the data shown in Fig. 1. The integral can be numerically calculated and thereby expressed in terms of C_1 and C_2. Accordingly, from the measured counting rates of the two moderated detectors, we can write the simultaneous equations

$$R_1 = k_{11} C_1 + k_{12} C_2 \tag{9a}$$

and

$$R_2 = k_{21} C_1 + k_{22} C_2, \tag{9b}$$

where k_{ij} is known and R_i is the observed counting rate ($i = 1, 2$; $j=1, 2$). Since for a moderated counter, neutrons produced in the moderator could contribute slightly to the counting rate, a correction must be made. The contribution is assumed to be proportional to the weight of the moderators. For the 2-1/2-in.-paraffin-moderated detector, 6% of the total counts was taken to be due to the local neutron production in the moderator, after the result obtained by Kent [1963].

The spatial and energy distributions of slow neutrons very near the ground are greatly affected by ground conditions in a complicated way. However, in approximating the thermal-neutron energy distribution by a Maxwellian, we can reasonably state that the thermal-neutron temperature near the ground is determined by the neutron-diffusion properties of the earth rather than of the air. This statement should be supported by the fact, to be shown later, that thermal neutrons near the ground come predominantly from the ground. In what follows, then, we assume a Maxwellian distribution with a certain neutron temperature for the thermal energy distribution near the ground.

B. Neutron Fluxes on the Ground

Measurements at 10 600 ft elevation were made about 1m above the dry ground with the detector axis parallel to the ground surface. At sea level, experiments were mainly conducted in a four-storied concrete building. Data were taken at each floor, as well as on the roof of the building. The building was a public garage in the City of Berkeley. The garage was so large and had such a low ceiling that the experiments in the building were considered to be a simulation of measurements at various depths in the ground. An advantage of the experiment is that the composition of the concrete can be taken as approximately that of the earth with constant moisture content. In the building, an unshielded BF_3 counter, a 9/10-in. polyethylene counter, and a 2-1/2-in. paraffin-moderated counter were operated simultaneously with about 1 m separation between them. The experimental results thus obtained are summarized in Table 5. The neutron fluxes determined from the counting rates are shown in Table 6. The fast-neutron fluxes were obtained by integrating Eq. (7). The total neutron fluxes from 0.4 eV to 10 MeV differ by only few percent when n in Eq. (7) changes from 1.16 to 1.74. It should be noted that since both the sensitivity of the moderated detectors and the flux intensity of the neutrons rapidly decrease above 10 MeV, neglect of the contribution from neutrons above 10 MeV to the counting rates does not introduce a significant error. Neutron energy spectra obtained are shown in Figs. 2 and 3 for the data taken on the dry ground at White Mt., and in the concrete-building.

To obtain the thermal-neutron flux from the counting rate of the slow-neutron detector, we assume that the thermal-neutron energy distribution is expressed by a Maxwellian with a neutron temperature of 1.75 T_0 (°K), where T_0, the temperature of the measuring location is taken as 293°K. This is discussed again in a later section. It should be noted that, in a well-diffusing medium, the neutron temperature approaches T_0, while in the free atmosphere it is found to be about $3T_0$, because of strong neutron capture by nitrogen. The intensity of the thermal-neutron flux obtained from the counting rate of the $1/v$ detector varies by a factor of $\sim \sqrt{3}$ when the neutron temperature changes from T_0 to $3T_0$.

Results of experiments in the parking garage are also shown in Fig. 4. After the transition region is passed, the slow-neutron counting rate decreases exponentially with depth. The exponential part of the curve could be accounted for by attenuation of the neutron-producing radiations. A rough estimate of 25 g/cm^2 for each thickness of the reinforced-concrete floor of the building yields an attenuation length of about 170 g/cm^2 for neutron-producing radiation. The counting rates measured by the moderated detectors seem to decrease more rapidly with concrete thickness near the roof until a secular equilibrium with the neutron-producing radiation is attained at the lower floors. The ratios of counting rates of the two moderated detectors taken on the roof and at each floor remained rather constant, indicating that the neutron energy spectrum does not change significantly on the roof and inside the building

It should be mentioned that in deriving the neutron flux intensities shown in Table 6 from the measured counting rates, an isotropic neutron flux distribution was assumed on the ground. However, as will be discussed later, this is not actually the case for both thermal and fast-neutron fluxes, especially for thermal neutrons. If anisotropy of the flux distribution is marked, and the sensitivity of the detector changes considerably with angle, a correction will be necessary for the measured counting rates, depending on the direction of detector axis. However, we will show later that anisotropy of the fast-neutron flux on the ground may be neglected.

C. Angular Distribution of Thermal Neutrons on the Ground

To obtain information on angular distribution of thermal neutrons on the ground, an experiment was performed at White Mt. (10 600 ft). A slow-neutron detector (bare BF_3 counter) was collimated by using a cone covered with a Cd sheet in such a way that the detector measured only those thermal neutrons that entered in a solid angle of $2\pi(1-\cos 66°)$ in a certain direction. A Cd collimator with a smaller solid angle was first made, but the counting rates with this collimator were too small to yield good statistics. Since the collimated solid angle used was comparatively large, data were taken for only two directions, upward and downward. The experimental results are shown in Table 7.

In accordance with the diffusion approximation [Glasstone and Edlund, 1952a] we express the angular distribution of thermal neutrons near the air-ground boundary by the first two terms of the spherical-harmonics expansion

$$F(x, \theta) = \frac{1}{2}\phi(x) + \frac{3}{2} J \cos\theta. \qquad (10)$$

Here $F(x, \theta)$ is the neutron flux through a ring element of area $2\pi \sin\theta d\theta$ with direction between θ and $\theta + d\theta$ at a distance x from the boundary. The total neutron flux is

$$\phi(x) = \int_0^{\pi} F(x, \theta) \sin\theta d\theta, \qquad (11)$$

and J is the neutron current through a unit area in the upward direction. The counting rate with the collimator is given by

$$R_1 = \frac{1}{2} \int_{\theta=0}^{66°} (\phi + 3J\cos\theta)\eta(\theta) \sin\theta d\theta \qquad (12)$$

for the downward direction and by

$$R_2 = \frac{1}{2} \int_{\pi-66°}^{\pi} (\phi + 3J\cos\theta)\eta(\theta) \sin\theta d\theta \qquad (13)$$

for the upward direction. Here $\eta(\theta)$ is the sensitivity of the detector at angle θ, being taken as unity at $\theta=0$ or π. Substituting $R_1 = 1.70$ and $R_2 = 2.69$ into Eqs. (12) and (13) and using the experimental results for the angular dependence of the detector's sensitivity, we obtain

$$\phi(x) = 8.44 \pm 0.35 \text{ n/sec} \tag{14a}$$

and

$$J = 0.882 \pm 0.160 \text{ n/cm}^2\text{-sec} \tag{14b}$$

on the ground. From the angular distribution obtained above, the total counting rate of the slow-neutron detector is

$$R = \int_0^\pi F(x, \theta)\, \eta(\theta) \sin\theta d\theta \tag{15}$$

$$= 6.17 \pm 0.26 \text{ cpm.}$$

This calculated result is in good agreement with the measured value, 6.53 ± 0.29 cpm.

In the vicinity of the air-earth boundary, the thermal-neutron flux at a distance x in g/cm^2 from the boundary is approximately

$$\phi(x) \simeq \phi(0) + x\, (d\phi/dx)_{x=0}, \tag{16}$$

where $(d\phi/dx)_{x=0}$ may be obtained by diffusion approximation:

$$J = -(1/6)\, (d\phi/dx)_{x=0} \left[\frac{1}{\Sigma_S(\text{earth})} + \frac{1}{\Sigma_S(\text{air})}\right]. \tag{17}$$

Here Σ_S(earth) and Σ_S(air) are the scattering cross sections of the earth and air, respectively. To obtain the scattering cross section, the composition of the earth was taken for the first approximation to be the same as the dry soil of the Nevada Test Site [Allen et al., 1963]. Substituting $J = 0.882$, $\Sigma_S(\text{air}) = 0.369\ cm^2/g$, and $\Sigma_S(\text{earth}) = 0.322\ cm^2/g$ into Eq. (17), we obtain $(d\phi/dx)_{x=0} = 0.91$ cpm per g/cm^2. These results indicate that the thermal-neutron flux in the ground increases rapidly with depth in such a way that it becomes twice the surface value at a depth of ~10 g/cm^2. This is in good agreement with the experimental results from the parking garage.

It should be noted that the thermal-neutron fluxes on the ground at 10 600 ft elevation and sea level, which were determined on the assumption of isotropic flux distribution, become about 15% higher than those shown in Table 6 when anisotropic flux distribution is considered.

4. DISCUSSION

A. Cosmic-Ray Neutron Production

Although many experiments on cosmic-ray neutron production rates have been made at various altitudes and latitudes, the results differ considerably. To compare our results with those reported previously, we briefly review the other results.

In the atmosphere, there is a small but significant amount of resonance capture of neutrons with energies above 0.5 MeV. Below this energy, the neutrons are captured predominantly by 1/v absorption. In the following, we discuss the number of neutrons that escape the resonance absorption and reach the 1/v region per second and per gram of air. For simplicity, we set this number equal to the neutron production rate, as in the foregoing discussion.

The experiments on the neutron production rate may be classified into three categories according to the experimental methods: first, measurement of slow neutrons in the free atmosphere; second, measurement of the neutron energy spectrum as well as the neutron flux intensities in the free atmosphere; and third, measurement of slow neutrons in a massive slowing-down medium on the ground.

Yuan [1951] measured the slow neutrons in the free atmosphere by means of the Cd-difference method by using calibrated BF_3 counters. The Cd-difference counting rates correspond to about half the rate of absorption of neutrons captured in the 1/v region [Anderson, 1953]. Davis [1950] used unshielded BF_3 counters in the free atmosphere which directly measured the neutron absorption rates in the 1/v region. As pointed out by Lattimore [1951], his results must be multiplied by a factor of 2.4 because he wrongly used a low value for the absorption cross section of air. Hess et al. [1959, 1961] experimentally determined the equilibrium neutron-energy spectrum, from which the neutron absorption rate in the 1/v region could be calculated. Newkirk [1963] calculated the neutron energy spectrum and used, as the source neutron intensities, the data obtained by Smith et al. [1961]. The neutron absorption rate in the 1/v region calculated from Newkirk's results agrees with that of Hess et al. in the equilibrium region, when the data are translated to the same geomagnetic latitude. Korff et al. [1948] made measurements at mountain altitude by surrounding a BF_3 counter with water-filled cans. Since the water moderator was thick enough, it is considered that the measurement was made in an equilibrium region in water. The results are recalculated in this paper by using newer cross section data for hydrogen and boron. Tobey et al. [1949] measured the neutron production rate in paraffin. However, since they employed nearly the same paraffin pile in dimension as we did at White Mt., the results may have been overestimated because of the significant contribution from external neutrons. Lattimore [1951] used boron-loaded nuclear emulsions to measure slow-neutron flux in massive ice at mountain altitude. Swetnick [1954] measured slow-neutron flux by the Cd-difference method at an equilibrium region in water, using an estimated neutron production rate. Although the data were not corrected for possible occurrence of the flux-depression effect around the detectors in water, the results would not be affected significantly. However, his results must be multiplied by a factor of 2 for the same reason as that for Davis [1950]. Experimental results were transferred to a geomagnetic latitude $\lambda = 44°$ N by using the experimental data of Simpson [1951] on the latitude variation of neutron intensity at about 300 g/cm^2 altitude, the data of Simpson and Fagot [1953] at about 680 g/cm^2 and the results of Rose et al. [1956] at sea level. Neutron capture by the reaction $^{16}O(n, \alpha)\,^{13}C$ (with a threshold energy of 2.3 MeV) is unimportant in air [Seitz and Huber, 1955]. However, it should be noted that neutrons produced in water are slowed down to the thermal region without significant loss. Therefore, if the same number of source neutrons is produced by cosmic rays in water and in the air, more neutrons should be captured in the $1/v$ region in water than in the air.

The absolute values of neutron production shown in Fig. 5 differ as much as a factor of 5 at the same altitude. In extending the exponential variation of the data of Hess et al. and Newkirk to sea level, we see that their results are larger by a factor of 3 than ours. The differences might be partly related to the time variation of cosmic-ray intensity associated with solar activity, although their effect is not thought to be appreciable at lower altitudes. Therefore we have no full explanation for these large discrepancies.

B. Neutron Fluxes at the Air-Ground Boundary

As described previously, neutron fluxes near the ground are not in equilibrium with the neutron-producing radiations. In what follows, we discuss air-ground boundary effects on the basis of the experimental data. One of the most prominent effects at the boundary should be a marked increase of earth-born thermal neutrons, by which we mean neutrons of energies below the Cd cutoff.

In the free atmosphere, where the neutron production rate is equal to the neutron absorption rate, we have

$$\Phi_{th} \cdot \hat{\Sigma}_{th,a} + \Phi_f \cdot \hat{\Sigma}_{f,a} = q, \tag{18}$$

where q is the rate of production of neutrons that escape resonance absorption and reach the 1/v region in n/g-sec, Φ_{th} is the thermal neutron flux below the Cd cutoff in n/cm^2-sec, Φ_f is the flux of fast neutrons of energies between the Cd cutoff and about 0.1 MeV in n/cm^2-sec, $\hat{\Sigma}_{th,a}$ is the effective absorption cross section for thermal neutrons in cm^2/g, and $\hat{\Sigma}_{f,a}$ is the effective absorption cross section for fast neutrons in cm^2/g. The absorption cross section in the energy region of interest may be expressed by the 1/v law for both thermal and fast neutrons. On the other hand, the Cd ratio is

$$R_{Cd} = \frac{\Phi_{th} \cdot \hat{\Sigma}_{th,a} + \Phi_f \cdot \hat{\Sigma}_{f,a}}{\Phi_f \cdot \hat{\Sigma}_{f,a}} . \tag{19}$$

From Eqs. (18) and (19), we obtain

$$\Phi_{th} = \frac{q}{\hat{\Sigma}_{th,a}} \cdot \frac{R_{Cd}-1}{R_{Cd}} . \tag{20}$$

Using a 1/v detector, Yuan [1951] found the Cd ratio in the free atmosphere to be 2.

Next, we estimate the effective absorption cross section of air for thermal neutrons, which is given by

$$\hat{\Sigma}_{th,a} = \frac{\int^{0.4\,eV} \phi_{th}(E)\, \Sigma_a(E)\, dE}{\int^{0.4\,eV} \phi_{th}(E)\, dE} , \tag{21}$$

where $\phi_{th}(E)$ is the thermal-neutron energy distribution and $\Sigma_a(E)$ is the absorption cross section at energy E. We also approximate the energy distribution of thermal neutrons in the free atmosphere by a Maxwellian with a shifted neutron temperature:

$$\phi_{th}(E) = \text{const} \cdot E \ \exp(-E/k\,T_n). \tag{22}$$

The shifted neutron temperature T_n is obtained by using the formula of Pool et al. [1958],

$$T_n = T\left(1 + 0.91 \sum_i a_i A_i \frac{\sigma_{a,i}}{\sigma_{S,i}}\right), \tag{23}$$

where T is the temperature of the medium in °K, a_i is the fraction of atoms of element i with an atomic weight A_i, $\sigma_{a,i}$ is the capture cross section evaluated at an energy kT, and $\sigma_{S,i}$ is the scattering cross section. Using the cross-section data given by Hughes and Schwartz [1958], we find T_n to be about 2.9 T in the free atmosphere. The capture cross section of air at an energy E(eV) is $\Sigma_a(E) = 0.0099\,E^{-1/2}$ cm^2/g. From these data we find $\hat{\Sigma}_{th,a}$ to be about 3.2×10^{-2} cm^2/g. Hence, from Eq. (20) the thermal-neutron flux in the free atmosphere is

$$\Phi_{th} = \frac{q}{3.2\times10^{-2}} \times \frac{1}{2} = 15.6\ q \quad [\text{n/cm}^2\text{-sec}]. \tag{24}$$

The same sort of discussion can be applied to the thermal-neutron fluxes in an equilibrium region in the earth. In this case, because the absorption cross section of earth materials is much smaller than that of air, the Cd ratio measured with a 1/v detector should be much greater than unity. This assumption leads to the following approximation for the thermal-neutron flux in the earth instead of Eq. (20):

$$\Phi_{th} = \frac{q}{\hat{\Sigma}_{th,a}}. \tag{25}$$

As a matter of fact, because of the considerable variety of earth compositions, particularly water content, the thermal-neutron energy distribution, and hence the value of $\hat{\Sigma}_{th,a}$ in the earth, should be variable.

To see the variance of the effective absorption cross sections of earth, we estimate the values of $\hat{\Sigma}_{th,a}$ for known-composition samples of Nevada Test Site soil with different moisture content [Allen et al., 1963]. The thermal-neutron energy distribution is again approximated by a Maxwellian with a shifted neutron temperature. The soil compositions, the corresponding neutron temperatures, and the effective absorption cross sections are shown in Table 8. From these data, the thermal-neutron fluxes in an equilibrium region in the specified soils are;

$$\begin{aligned} \Phi_{th} &= 355\ q \quad \text{(in dry soil)} \\ &= 322\ q \quad \text{(in 50\% water-saturated soil)} \\ &= 235\ q \quad \text{(in 100\% water-saturated soil).} \end{aligned} \tag{26}$$

Note that the equilibrium thermal-neutron flux is greater in the soil with smaller moisture content because of the higher absorption cross section of hydrogen. The altitude variation of the neutron production rate in air, q, expressed by an exponential function, may be extended into the earth by multiplying by a factor of 1.1 to correct for an increase in the neutron production rate in earth as mentioned previously.

It is quite difficult to predict the exact thermal flux intensity near the air-ground boundary. However, it seems reasonable to assume, from experimental results, that the thermal-neutron flux should be in equilibrium with the neutron production rate at a distance from the boundary of more than 5 mean free paths (about 100 m in air at sea level and about 15 to 20 cm in the earth). The thermal-neutron fluxes near the boundary are graphically estimated in Fig. 6 by connecting the equilibrium thermal-neutron fluxes in the air and the earth. The thermal-neutron flux intensity near the boundary thus is obtained for Nevada dry soil. The slope of the curve near the boundary may be taken from experimental results. It should be noted, however, that the energy distribution of thermal neutrons changes with distance from the boundary, varying in such a way that the energy spectrum is hardened with elevation in the air to approach the equilibrium spectrum. Also, the fast-neutron flux near the air-ground boundary is not in equilibrium with the neutron production rate. In an equilibrium region both in air and in earth, if we use the slowing-down theory and neglect resonance absorption in the process, the fast-neutron energy spectrum in n/cm^2-sec-MeV in the energy region below 0.1 MeV can be approximated by

$$\phi(E) = \frac{q}{\xi \Sigma_S} \cdot \frac{1}{E} \quad , \tag{27}$$

where q is the rate of production of neutrons that escape resonance absorption and reach the 1/v region in n/g-sec, and $\xi \Sigma_S$ is the slowing power in cm^2/g. The slowing power for air (80% N_2 + 20% O_2) is found to be 5.167×10^{-2} cm^2/g. For Nevada soils, it is shown in Table 8. Since possible boundary effects might occur within a distance from the boundary of the order of the root-mean-square distance necessary to slow neutrons to thermal energies from an initial energy of a few MeV, Eq. (27) should be valid only beyond this distance from the boundary. The root-mean-square distance traveled by a neutron in being slowed down from 2 MeV to 1 eV, calculated from Fermi age theory [Glasstone and Edlund, 1952, p. 181] is found to be about 90 g/cm^2 in air and about 52 g/cm^2 in Nevada dry soil. In the vicinity of the boundary, the fast-neutron flux intensities can be graphically evaluated in the same way as for thermal neutrons, by connecting the equilibrium fast-neutron fluxes in the air and in the earth. The fast-neutron fluxes thus estimated near the boundary are shown in Fig. 7. for Nevada dry soil. It can be seen from Fig. 7 that the fast-neutron flux near the boundary is lower than the value expected from the exponential variation in the free atmosphere. The experimental results of the fast neutron fluxes obtained in the concrete building as shown in Fig. 4 are thus explained by the boundary effect demonstrated above. The equilibrium-energy spectrum for fast neutrons should not be much affected at the boundary, since the deviation from a 1/E spectrum below 0.1 MeV is not appreciable and the error in the measured fast-neutron fluxes introduced by assuming a 1/E spectrum would be of the order of the experimental error.

C. Comparison of the Calculated and Measured Neutron Fluxes at the Air-Ground Boundary

In the foregoing section, we have discussed the possible air-ground boundary effects on the slow and fast-neutron fluxes simply but rather quantitatively. Although there are still several uncertainties, we now compare the measured neutron fluxes to those calculated by using the neutron-production data. We assume that the compositions of the dry soil at White Mountain and of the concrete of the parking garage are similar to that of the Nevada Test Site dry soil. The spatial and energy distribution of thermal neutrons at the boundary is assumed to be such that the neutron temperature is 1.75 T_0 and that the flux is isotropic. It is unlikely that the error of the thermal-neutron flux intensity determined on these assumptions exceeds 50%. The fast-neutron flux is calculated by integrating Eq. (27) from 0.4 eV to 0.1 MeV. In this case, we use 5.167×10^{-2} and 1.60×10^{-1} cm^2/g as the slowing power of air and soil respectively; hence two different results are obtained. The measured fast-neutron flux should be between the two calculated values. For the neutron production rate, we use our experimental results measured in water, that is, $q = 1.28 \times 10^{-4}$ n/g-sec at 10 600 ft elevation and $q = 1.85 \times 10^{-5}$ n/g-sec at sea level. It should be noted that the total neutron production rates are slightly higher in air than in water, as shown in Table 2. However, in the air a small but significant number of neutrons are lost due to resonance absorption before the initially produced neutrons can reach the energy region below 0.1 MeV. According to Anderson [1953], the probability that a 2-MeV neutron can reach the energy region below 0.1 MeV without capture is 0.86 in the free atmosphere. Therefore, the rate of production of neutrons that can reach the energy region below 0.1 MeV is slightly lower in air than in water. A comparison of the measured and calculated fluxes is shown in Table 9.

From the calculated fluxes in both air and soil, the probable neutron flux on the ground can be estimated by using the curve of neutron flux variation near the air-ground boundary, which is shown in Figs. 6 and 7. As shown in Table 9, the measured and calculated neutron fluxes are in a good agreement except the fast-neutron flux at 700 g/cm^2 elevation. That the calculated fast-neutron flux at 700 g/cm^2 is lower than that measured seems to be due to the fact that the measured neutron production rate at 700 g/cm^2 elevation is lower by a factor of 0.7 than the value expected from the data at sea level and an exponential variation with a mean free path of 145 g/cm^2. We believe our experimental data on the neutron production rate at sea level are more reliable than those taken at 700 g/cm^2. In conclusion, we feel that our experimental results reported in this paper are the most reliable data available on the cosmic-ray neutron production rate and fluxes at sea level for the period of minimum solar activity.

5. CONCLUSIONS

(i) The flux intensity of the cosmic-ray neutrons on the ground at a geomagnetic latitude 44° N was determined by using well-calibrated neutron counters. The thermal-neutron flux intensity was found to be 1.07×10^{-3} n/cm^2-sec on the roof of a four-storied building at sea level and 1.20×10^{-2} n/cm^2-sec on dry ground at 700 g/cm^2 elevation, with an estimated error of less than 50%. This error arises mainly from the uncertainty of the energy distribution of the thermal neutrons. From the data obtained by using two differently moderated counters, the neutron energy spectrum was established in the energy range about 1 eV to 10 MeV. The energy spectrum does not show a sharp bump due to neutron evaporation around 1 MeV as that reported by Hess et al. [1959]; it is very similar to the spectrum for the free atmosphere calculated by Newkirk [1963].

From the energy spectrum obtained, the fast-neutron flux was found with an estimated error of better than 10%. On the roof of a four-storied building at sea level, the fluxes were 219×10^{-3} n/cm^2-sec at 0.4 to 10^5 eV, 1.6×10^{-3} n/cm^2-sec at 0.1 to 1 MeV, and 1.7×10^{-3} at 1 to 10 MeV; on dry ground at 700 g/cm^2 elevation, they were 3.8×10^{-2} n/cm^2-sec at 0.4 to 10^5 eV, 1.9×10^{-2} at 0.1 to 1 MeV, and 1.7×10^{-2} n/cm^2-sec at 1 to 10 MeV.

(ii) The knowledge of the absolute rate of neutron production would help us understand the local variation of the neutron-flux intensity on the ground and to confirm the realiability of the measured neutron fluxes.

Because of absence of quantitative data for neutron production rates at sea level except that of Tobey et al. [1949, 1951], we tried to measure the cosmic-ray neutron production rate in a massive paraffin pile and in water. For the paraffin pile, the neutrons produced outside the pile significantly contributed to the counting rate of the neutron counter embedded in the pile; therefore, our data taken in the paraffin pile were abandoned. Also, the reported data taken by Tobey et al. in nearly the same size paraffin pile must be corrected for the external neutron contribution. The experimental results determined in water yield a neutron-production rate of 1.85×10^{-5} n/g-sec in water at sea level, with an estimated error of about 10%.

(iii) In order to correlate the neutron-production rate with the neutron fluxes on the ground, the approximate profile pictures of slow- and fast-neutron distribution near the ground were made semiquantitatively for the case of Nevada Test Site ground with different water contents. Experimental results obtained in a concrete building justify the approximate profile picture of the neutron distribution near the boundary. It is shown that both the thermal- and fast-neutron fluxes on the ground decrease when the water content of the soil increases. It should be of interest to note here that Gorshkov et al. [1964] recently reported their findings that the slow-neutron flux on the ground is more than 3.1 times that over water bodies.

The measured neutron fluxes are compared with the calculated fluxes from the neutron production rate. They are in agreement when we take into account the uncertainty of the neutron diffusion properties of the surrounding media where the neutron fluxes were measured.

(iv) Anisotropy of the thermal-neutron flux on the ground was measured, and the angular distribution was well fitted by the first two terms of a spherical-harmonics expansion. When this anisotropic flux distribution is considered, the thermal-neutron flux on the ground at 700 g/cm^2 elevation, which was determined on the assumption of isotropic flux distribution, becomes about 15% higher. It can be shown that anisotropy of fast-neutron flux on the ground is very small.

ACKNOWLEDGMENT

We wish to thank Dr. Nobuo Oda for his helpful criticism and suggestions on the experiments, and Mr. Alan R. Smith for his helpful discussion. We also thank Mr. C. E. Wilson and other crew members of the High Altitude Research Station, University of California, at White Mountain, California for their warm hospitality during the experiments, as well as their kind permission to use the atmospheric-pressure data. Thanks are due the members of the Dewing Park Recreation Club of Walnut Creek, California, who kindly allowed us to use their private swimming pool.

One of the authors (M. Yamashita) was financially supported by the Atomic Energy Research Fellowship of the Government of Japan. He wishes to express his thanks to Dr. Hironobu Watanabe, who kindly let him have time to prepare this manuscript at the National Institute of Radiological Sciences, Japan.

This work was done under the auspices of the U. S. Atomic Energy Commission.

REFERENCES

Allen, F. J., A. Futterer, and W. Wright, Neutron reflection and flux versus depth for Nevada Test Site soil, Ballistics Research Laboratory Report BRL-1190, 1963.

Anderson, E. C., The production and distribution of natural radio carbon, Ann. Rev. Nucl. Sci., 2, 63-78, 1953.

Bethe, H. A., S. A. Korff, and G. Placzek, On the interpretation of neutron measurements in cosmic radiation, Phys. Rev., 57, 573-587, 1940.

Boella, G., G.D. Antoni, C.Dilworth, G. Giannelli, E. Rocca, L. Scarsi, and D. Shapiro, Measurement of the cosmic-ray neutron flux in the atmosphere, Nuovo Cimento, 29, 103-117, 1963.

Brown, W. W., Cosmic-ray nuclear interactions in gases, Phys. Rev., 93, 528-534, 1954.

Davis, W. O., Energy and density distribution of cosmic-ray neutrons, Phys. Rev., 80, 150-154, 1950.

Draper, J. E., Evaluation of neutron counter efficiency, Nucleonics, 6, 32-40, 1950.

Edge, R. D., The altitude dependence of atmospheric cosmic-ray neutrons and the slow neutron density below a water surface, Nucl. Phys. 12, 182-189, 1959.

Geiger, K. W., Evaporation neutrons from cosmic ray nuclear interactions in various elements, Can. J. Phys. 34, 288-303, 1956.

Glasstone, S., and M. C. Edlund, The elements of nuclear reactor theory, D. Van Nostrand, New York, 1952 (a) p. 389 (b) p. 181.

Gorshkov, G. V., V. A. Eyabkin, and O. S. Tsvetkov, On neutron background at the Earth's surface, Atomnoya Energia 17, 492-496 (1964).

Hess, W. N., E. H. Canfield, and R. E. Lingenfelter, Cosmic-ray neutron demography, J. Geophys. Res., 66, 665-677, 1961.

Hess, W. N., H. W. Patterson, and R. Wallace, Cosmic-ray neutron energy spectrum, Phys. Rev. 116, 445-457, 1959.

Hughes, D. J., and R. Schwartz, Neutron cross sections, Brookhaven National Laboratory Report BNL-325 Second Ed., 1958.

Kastner, J. B., B. G. Oltman, and L. D. Marinelli, Progress report on flux and spectrum measurements of the cosmic-ray neutron background, "Natural Radiation Environment." pp 441-482 (1964).

Kent, R. A. R., Cosmic-ray neutron measurement, Hanford Works Report HW-SA 2870, 1963.

Korff, S. A., and A. Cobas, The production of nucleons by cosmic radiation, Phys. Rev., 73, 1010-1014, 1948.

Ladenburg, R., The absorption rate of cosmic-ray neutrons producing C^{14} in the atmosphere, Phys. Rev., 86, 128, 1952.

Lattimore, S., Rate of production of neutrons in ice by cosmic rays, Phil. Mag., 42, 331-337, 1951.

Lattimore, S., Calculations on the number of neutrons in the atmosphere, Phys. Rev., 81, 643, 1951.

Lingenfelter, R. E., and E. J. Flamm, Solar neutrons and the earth radiation belts, Science, 144, 292-294, 1964.

Mendell, R. B., and S. A. Korff, Fast neutron flux in the atmosphere, J. Geophys. Res., 68, 5487-5495, 1963.

Miyake, S., K. Hinotani, and K. Nunogaki, Intensity and energy spectrum of fast neutrons in cosmic radiation, J. Phys. Soc. Japan, 12, 113-121, 1957.

Newkirk, L. L., Calculation of low energy neutron flux in the atmosphere by the Sn method, J. Geophys. Res., 68, 1825-1833, 1963.

Ortel, W. C. G., Neutron production by cosmic rays, Phys. Rev., 93, 561-567, 1954.

Patterson, H. W., and R. Wallace, A method of calibrating slow-neutron detectors, Lawrence Radiation Laboratory Report UCRL-8395, 1958, unpublished.

Poole, M. J., M. S. Nelkin, and R. S. Stone, The measurement and theory of reactor spectra, in Progress in Nuclear Energy, Series 1, Phys. and Mathematics Vol. 2, pp. 91-164, Pergamon Press, New York, 1958.

Rose, D. C., K. B. Fenton, J. Katzman, and J. A. Simpson, Latitude effect of the cosmic-ray nucleon and meson components at sea level from the arctic to the antarctic, Can. J. Phys., 34, 968-984, 1956.

Seitz, J., and P. Huber, Wirkungsquerschnitt der $O^{16}(n,\alpha)C^{13}$ reaktion für schnelle neutronen, Helv. Phys. Acta, 28, 227-244, 1955.

Simpson, J. A., W. Fonger, and S. B. Treiman, Cosmic radiation intensity-time variations and their origin. 1. Neutron intensity variation method and meteorological factors, Phys. Rev., 90, 934-950, 1953.

Simpson, J. A., and R. B. Uretz, Cosmic ray neutron production in elements as a function of latitude and altitude, Phys. Rev., 90, 44-50, 1953.

Simpson, J. A., Neutrons produced in the atmosphere by the cosmic radiations, Phys. Rev., 83, 1175-1188, 1951.

Simpson, J. A., and W. C. Fagot, Properties of low-energy nucleonic components at large atmospheric depths, Phys. Rev., 90, 1068-1072, 1953.

Smith, R. V., L. F. Chase, W. L. Imhof, J. B. Reagan, and M. Walt, Radiation measurments with balloons, Armour Research Laboratory Report ARL-TDR-62-2, 1961.

Swetnick, M. J., Cosmic-ray neutrons in water at an altitude of 10 600 feet, Phys. Rev., 95, 793-796, 1954.

Tobey, A. R., Neutron production by cosmic rays, Phys. Rev., 75, 894-895, 1949.; Tobey, A. R., and C. G. Montgomery, Neutron production by cosmic rays at sea level, Phys. Rev., 81, 517-522, 1951.

Tongiorgi, V. C., On the mechanism of production of the neutron component of the cosmic radiation, Phys. Rev., 76, 517-526, 1949.

Yamashita, M., L. D. Stephens, A. R. Smith, and H. W. Patterson, Detection efficiency of bare and moderated BF_3-gas-filled proportional counters for isotropic neutron fluxes, Lawrence Radiation Laboratory Report UCRL-16103, 1965, unpublished.

Yuan, L. C. L., Distribution of slow neutrons in free air atmosphere up to 100 000 feet, Phys. Rev., 81, 175-184, 1951.

Table 1. Summary of experimental data on cosmic-ray neutron production rates in water and paraffin.

	Water	Paraffin
At 10 600 ft		
Background counting rate, BF_3 counter (cpm)	0.710 ± 0.020	0.710 ± 0.020
Net counting rate,* Cd difference (cpm)	2.46 ± 0.14	5.19 ± 0.18
Neutron production rate (n/g-sec)	$(9.38 \pm 0.45) \times 10^{-5}$	$(2.82 \pm 0.1) \times 10^{-4}$
Corrected rate† (n/g-sec)	$(1.28 \pm 0.06) \times 10^{-4}$	
At sea level		
Background counting rate, BF_3 counter (cpm)	0.682 ± 0.015	0.708 ± 0.013
Net counting rate,* Cd difference (cpm)	0.327 ± 0.029	0.267 ± 0.022
Neutron production rate, (n/g-sec)	$(1.25 \pm 0.11) \times 10^{-5}$	$(1.45 \pm 0.12) \times 10^{-5}$
Corrected rate† (n/g-sec)	$(1.85 \pm 0.16) \times 10^{-5}$	

* Corrected for barometric pressure.

† Corrected for attenuation of neutron-producing radiation in water.

Table 2. Relative rate of production of cosmic-ray neutrons in various media.

Medium	Density (g/cm^3)	Relative production rate (n/g)
Water, H_2O	1	1.000
Paraffin, $(CH_2)_n$	0.90	0.876
Air, $4N_2+O_2$		1.087
Earth, SiO_2		1.233

Table 3. Effect of external neutrons on the 60- by 69- by 96-cm paraffin pile. The systematic error of the experiment was estimated to be better than 10%. Isotropic distribution is assumed.

Source	Neutron energy (MeV)	Neutron flux (10^6 n/sec)	Counting rate ($cpm/n\text{-}cm^{-2}\text{-}sec^{-1}$)
Pu-Be	4.2	1.56	108
Po-mock fission	1.5	0.2145	68
Pu-Li	0.4	2.579	21

Table 4. Comparison of the reported neutron energy spectra approximated by E^{-n} in the energy range from 1 to 10 MeV.

n	Reference
1.16	Mendell et al. [1963]
1.24	Newkirk [1963]
1.25	Miyake et al. [1957]
1.74	Hess et al. [1961]

Table 5. Experimental results on slow- and fast-neutron fluxes on the ground at 700 g/cm^2 elevation and at sea level, geomagnetic latitude λ = 44° N.

Elevation	Measured counting rate, background substracted (cpm)		
	Bare BF_3 counter (Cd difference)	0.9-in.-polyethylene-moderated counter	2-1/2-in.-paraffin-moderated counter
Sea level			
On the roof	0.579±0.030	1.56±0.048	2.02±0.054
Fourth floor	1.010±0.034	1.23±0.045	1.77±0.053
Third floor	0.862±0.033	0.837±0.043	1.12±0.049
Second floor	0.755±0.042	0.756±0.052	1.03±0.065
First floor	0.637±0.031	0.586±0.040	0.726±0.046
On wet ground			1.54±0.04
700 g/cm^2			
On dry ground	6.53 ± 0.29	19.4 ± 0.65	24.0 ± 0.45

Table 6. Slow- and fast-neutron fluxes on dry ground at 700 g/cm^2 elevation and on a building roof at sea level. Fluxes were measured at a geomagnetic latitude λ = 44° N.

Neutron energy range (eV)	Neutron flux (n/cm^2-sec)							
	Fast neutrons*						Thermal nuetrons†	
	Sea level			700 g/cm^2			Sea level	700 g/cm^2
	n=1.16	1.24	1.74	1.16	1.24	1.74		
0.4-10^5	2.99×10^{-3}	2.95×10^{-3}	2.79×10^{-3}	3.92×10^{-2}	3.88×10^{-2}	3.72×10^{-2}		
10^5-10^6	1.50×10^{-3}	1.52×10^{-3}	1.68×10^{-3}	1.83×10^{-2}	1.86×10^{-2}	2.02×10^{-2}		
10^6-10^7	1.80×10^{-3}	1.78×10^{-3}	1.63×10^{-3}	1.74×10^{-2}	1.79×10^{-2}	1.64×10^{-2}		
Total	6.29×10^{-3}	6.25×10^{-3}	6.10×10^{-3}	7.49×10^{-2}	7.53×10^{-2}	7.38×10^{-2}	$1.07\pm0.055 \times10^{-3}$	$1.20\pm0.05 \times10^{-2}$

* Estimated error < 10%.

† The error term is based on the counting error only.

Table 7. Angular distribution of thermal neutrons on the ground. The Cd-difference counts give the contribution from thermal neutrons below 0.4 eV.

Condition	Counting rate (cpm)
Without collimator	8.21 ± 0.28
Covered with Cd sheet	1.68 ± 0.077
Cd difference	6.53 ± 0.29
With collimator	
Upward (Cd difference)	1.70 ± 0.13
Downward (Cd difference)	2.69 ± 0.12

Table 8. Composition of Nevada Test Site soil. Data are taken from Allen et al. [1963]. The corresponding neutron temperature and the effective absorption cross section for the thermal-neutron flux are calculated from Eqs. (23) and (21) respectively.

	Soil moisture		
	Dry	50% water-saturated	100% water-saturated
Element (atoms/cm^3)			
H	8.553×10^{21}	9.820×10^{21}	16.87×10^{21}
O	22.68×10^{21}	23.30×10^{21}	27.00×10^{21}
Al	2.014×10^{21}	1.830×10^{21}	1.976×10^{21}
Si	9.533×10^{21}	8.680×10^{21}	8.963×10^{21}
Density (g/cm^3)	1.15	1.12	1.25
Neutron temperature (°K)	1.73 T_0	1.65 T_0	1.54 T_0
Effective absorption cross section (cm^2/g)	2.82×10^{-3}	3.11×10^{-3}	4.26×10^{-3}
Slowing power (cm^2/g)	1.60×10^{-1}	1.87×10^{-1}	2.82×10^{-1}

Table 9. Comparison of measured and calculated neutron fluxes on the ground.

Elevation (g/cm^2)	Neutron energy (eV)	Calculated flux (n/cm^2-sec)		Measured flux (n/cm^2-sec)
		Medium	Flux	
700	$0.4-10^5$	Air	3.05×10^{-2}	$3.82\pm0.10\times10^{-2}$
		Soil	9.86×10^{-3}	
	≤ 0.4	Air	2.00×10^{-3}	$1.20\pm0.05\times10^{-2}$
		Soil	4.75×10^{-2}	
Sea level	$0.4-10^5$	Air	4.41×10^{-3}	$2.90\pm0.10\times10^{-3}$
		Soil	1.43×10^{-3}	
	≤ 0.4	Air	2.89×10^{-4}	$1.07\pm0.06\times10^{-3}$
		Soil	6.60×10^{-3}	

FIGURE LEGENDS

Fig. 1. Response of the moderated counters with neutron energy for isotropic neutron flux.

Fig. 2. Differential neutron energy spectrum measured on the dry ground at 700 g/cm^2 elevation.

Fig. 3. Differential neutron energy spectrum measured on the the roof of a concrete building at sea level.

Fig. 4. Variation of counting rate of the neutron detectors in a concrete building.

Fig. 5. Absolute rate of cosmic-ray neutron production, normalized at geomagnetic latitude $\lambda = 44°$ N.
(1) Korff et al. [1948] in water, (2) Swetnik [1954] in water,
(3) Tobey et al. [1949, 1951] in carbon, (4) Davis [1950] in air,
(5) Yuan [1951] in air, (6) Lattimore [1951] in ice,
(7) Hess et al. [1959, 1961] in air, (8) Newkirk [1963] in air,
(9) Yamashita et al. [1965] in water.

Fig. 6. Approximated picture of thermal-neutron flux intensity near the air-ground boundary. The neutron-production rate is taken as unity in the air at sea level.

Fig. 7. Approximate picture of fast-neutron flux per unit energy interval below 0.1 MeV near the air-ground boundary. The neutron production rate is taken as unity in the air at sea level.

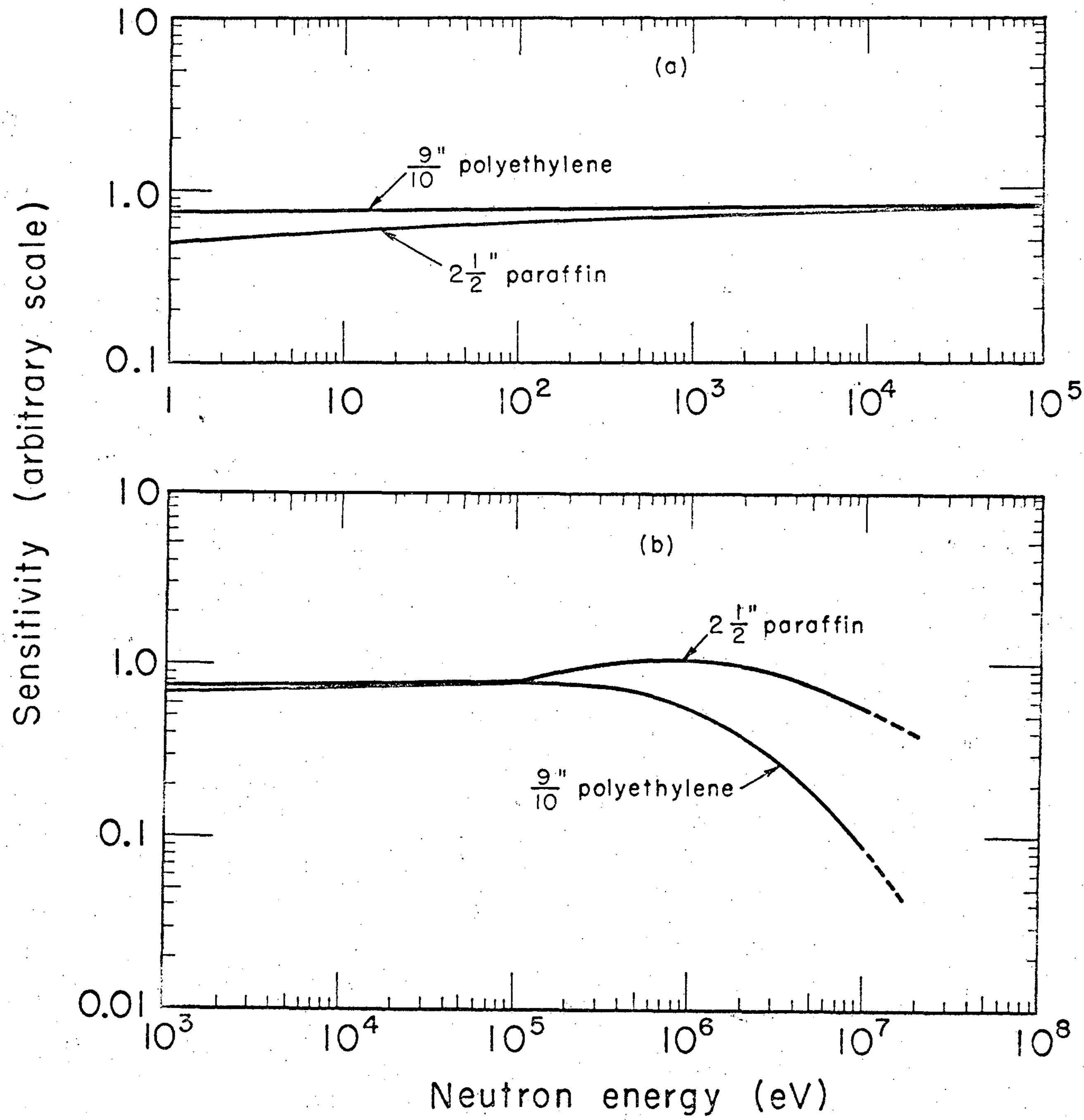

Fig. 1

MUB-6229

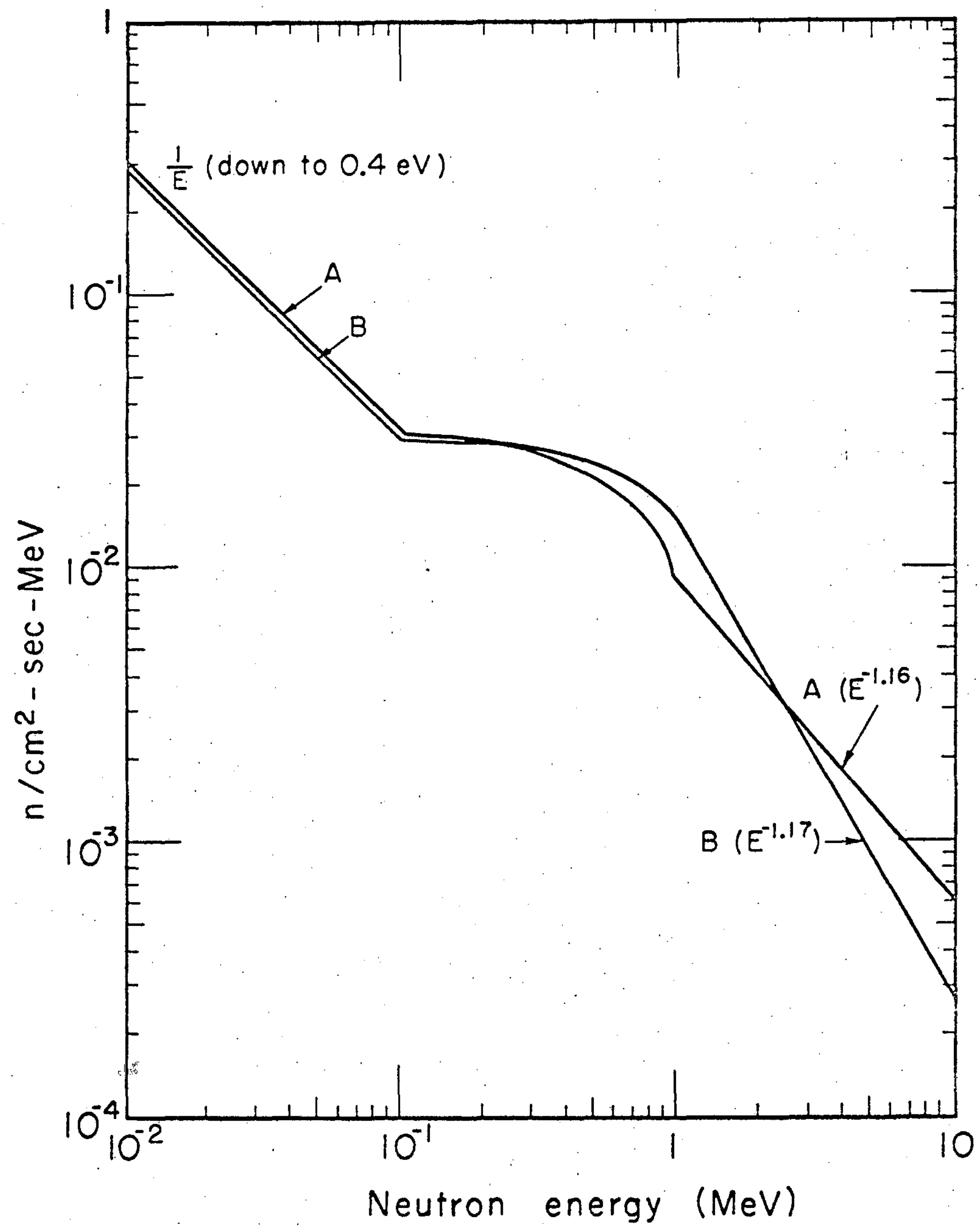

Fig. 2

MUB-6230

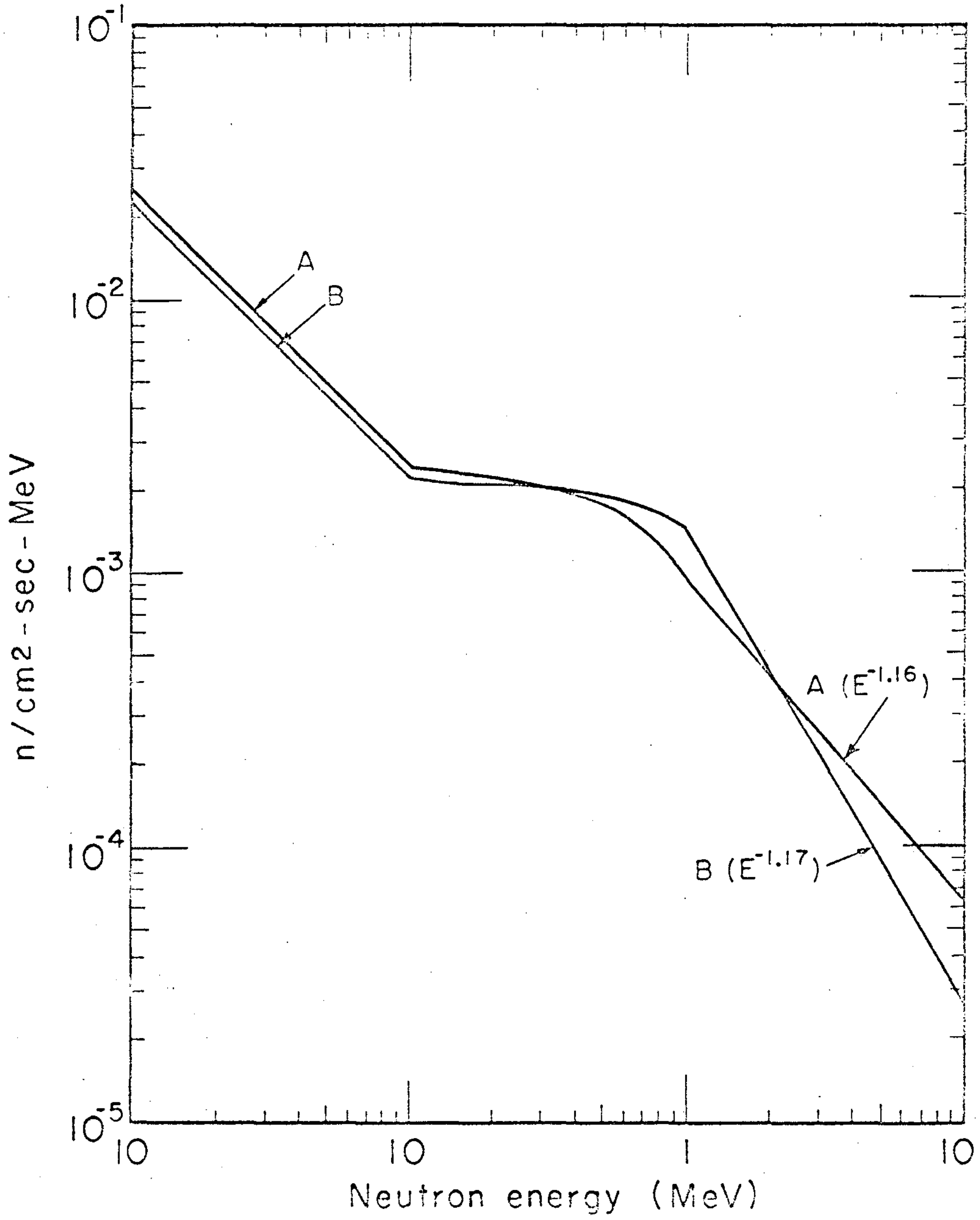

Fig. 3

MUB-6231

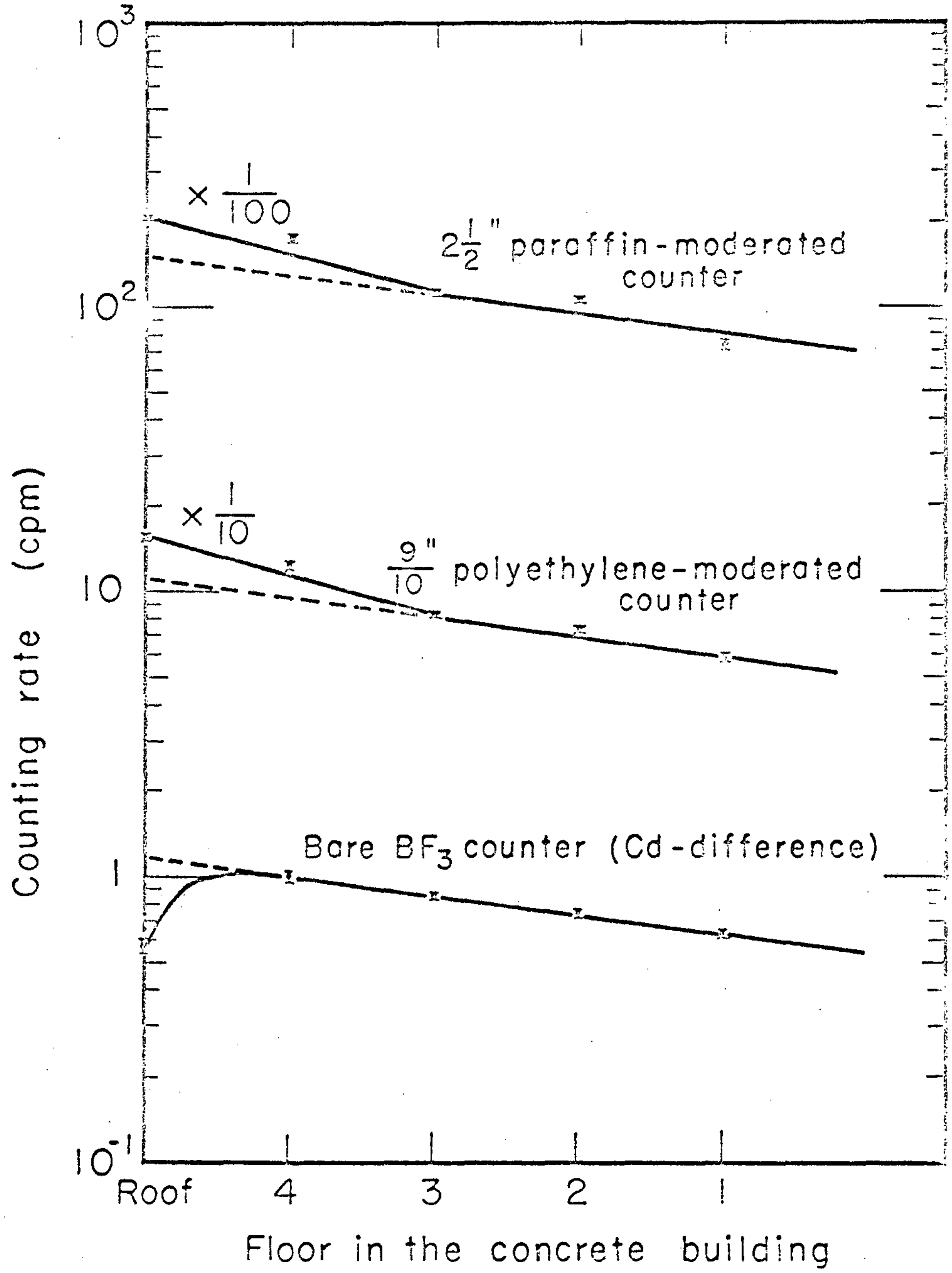

Fig. 4 MUB-6232

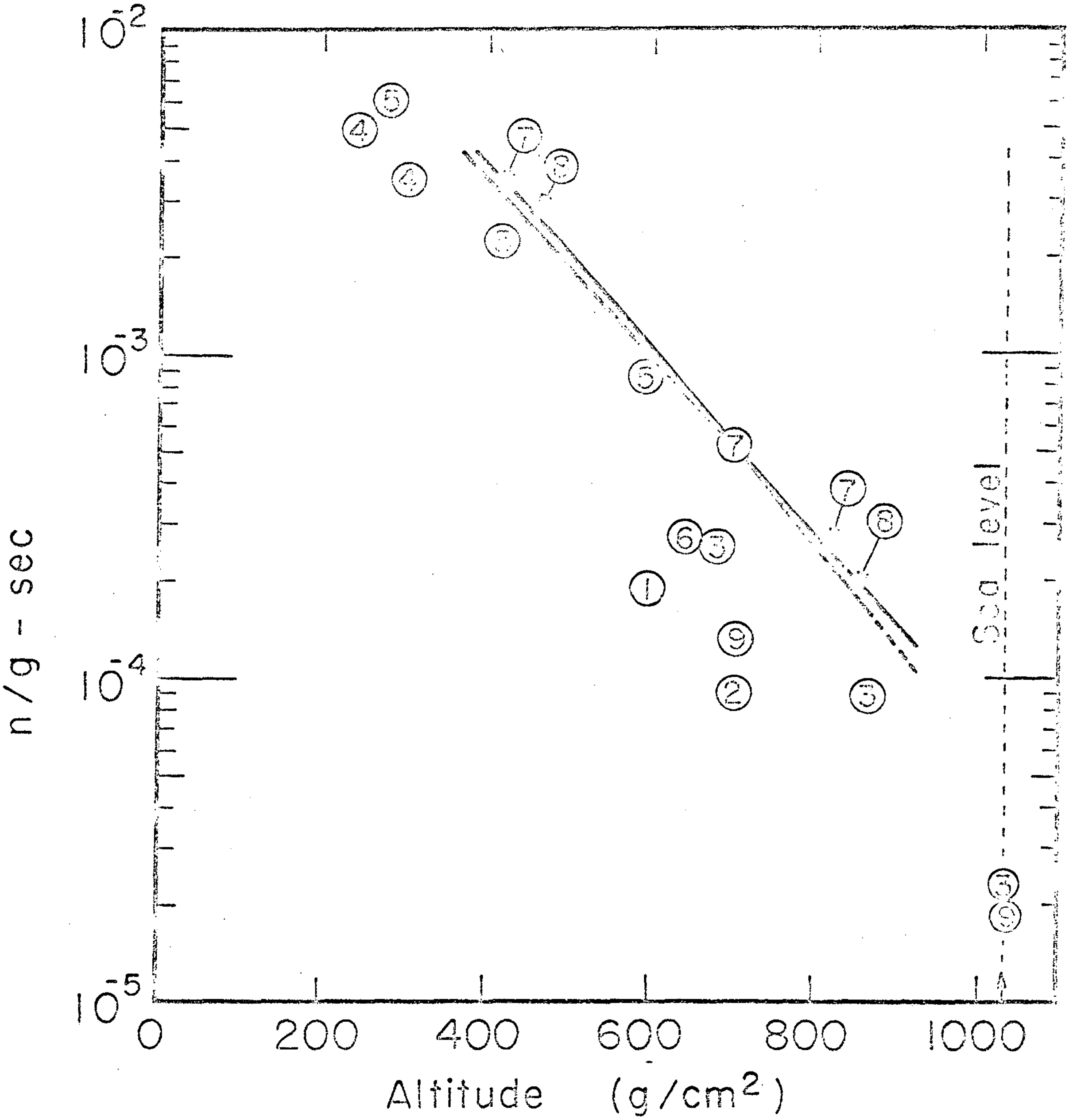

Fig. 5

MUB-6233

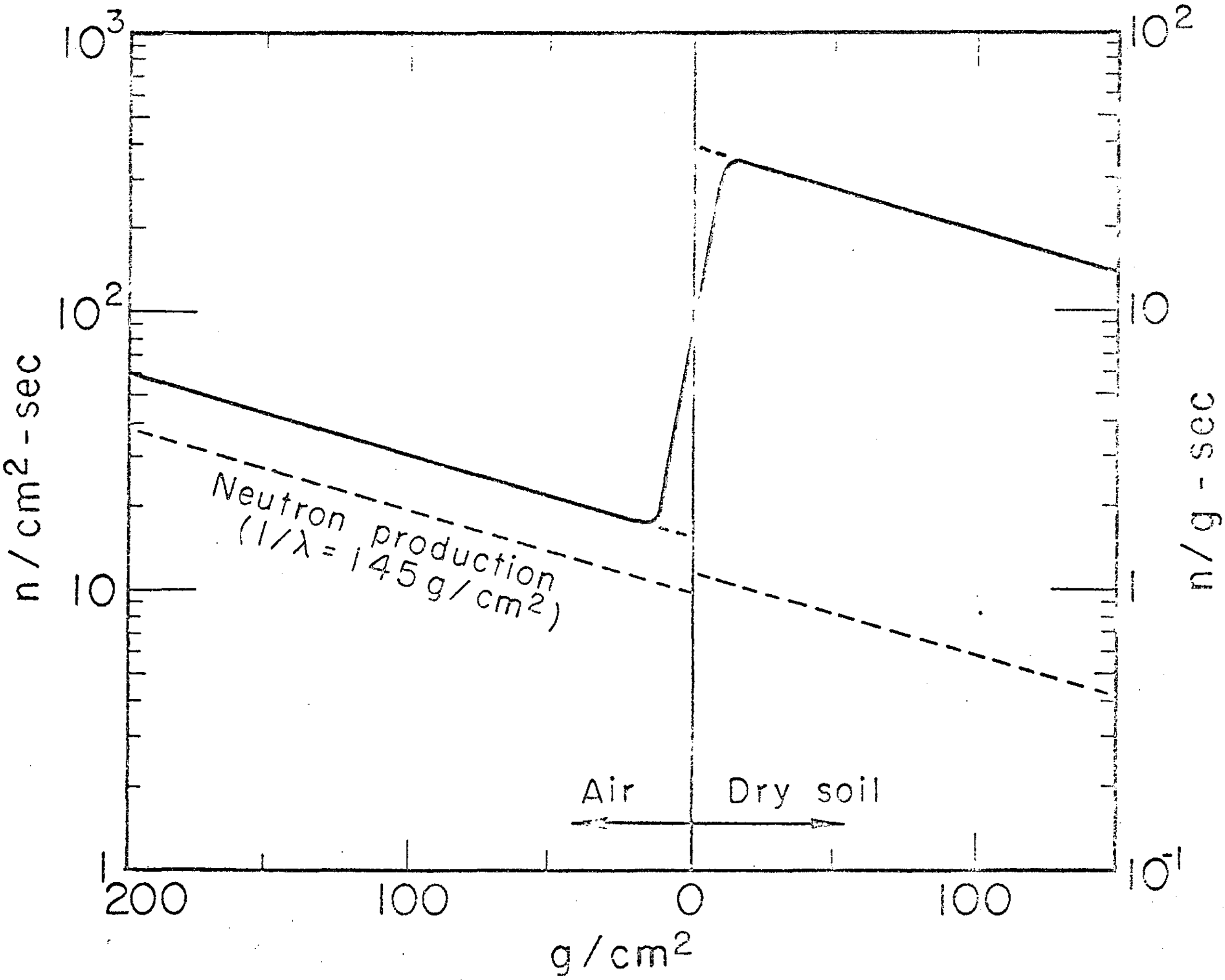

Fig. 6

MUB-6234

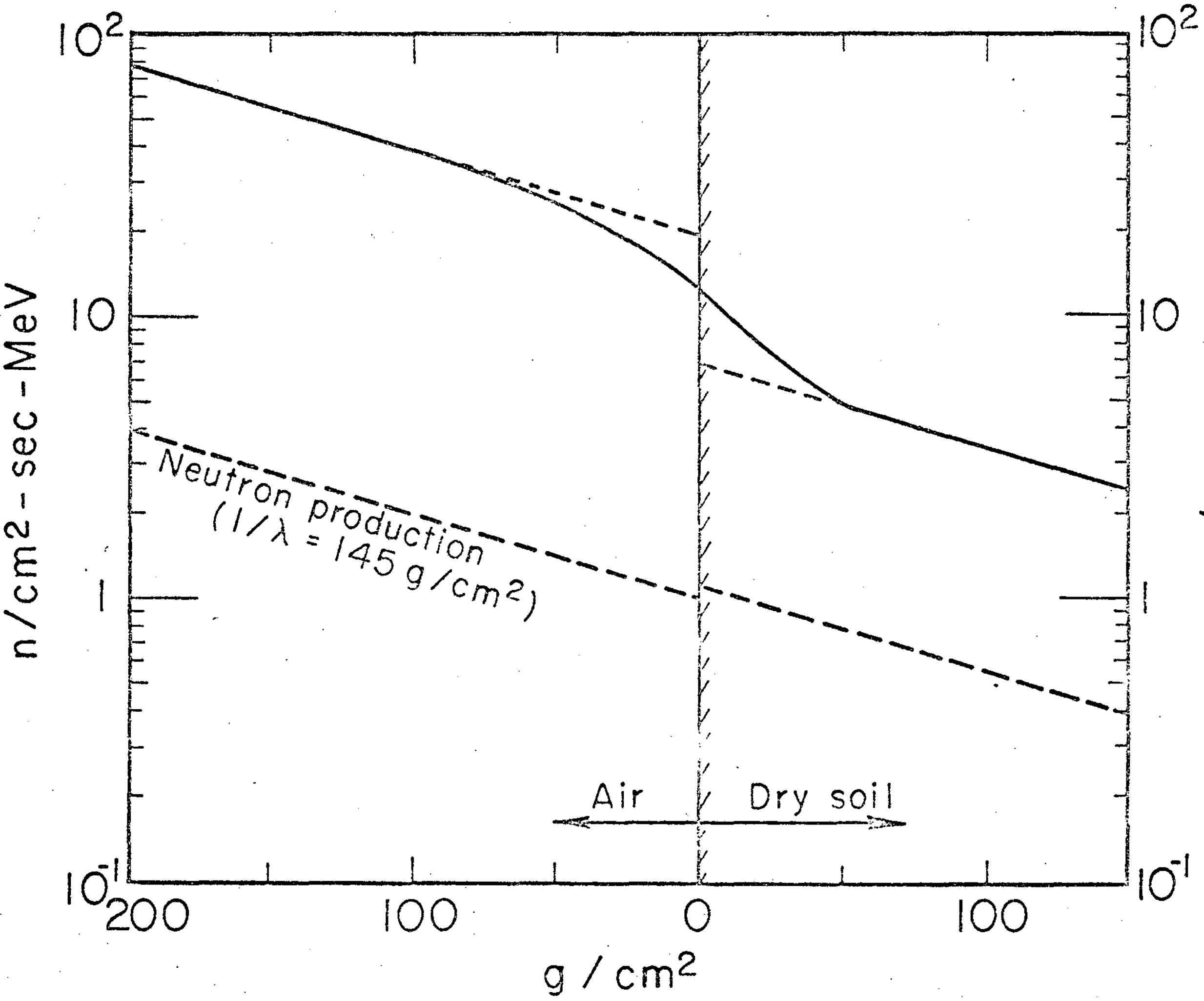

Fig. 7

MUB-6235